

Long-term stability of GaAs/AlAs terahertz quantum-cascade lasers

Cite as: AIP Advances **12**, 085122 (2022); <https://doi.org/10.1063/5.0098782>

Submitted: 12 May 2022 • Accepted: 04 August 2022 • Published Online: 29 August 2022

 L. Schrottke,  X. Lü,  K. Biermann, et al.



View Online



Export Citation



CrossMark

ARTICLES YOU MAY BE INTERESTED IN

[Increasing the output power of a heavily doped terahertz quantum cascade laser by avoiding the subband misalignment](#)

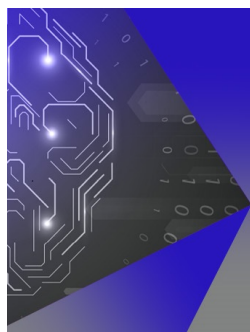
Journal of Applied Physics **132**, 173101 (2022); <https://doi.org/10.1063/5.0106751>

[Silicon integrated terahertz quantum cascade ring laser frequency comb](#)

Applied Physics Letters **120**, 091106 (2022); <https://doi.org/10.1063/5.0078749>

[Electromagnetic modeling of terahertz quantum cascade laser waveguides and resonators](#)

Journal of Applied Physics **97**, 053106 (2005); <https://doi.org/10.1063/1.1855394>



APL Machine Learning

Machine Learning for Applied Physics
Applied Physics for Machine Learning

**First Articles
Now Online!**

Long-term stability of GaAs/AlAs terahertz quantum-cascade lasers

Cite as: AIP Advances 12, 085122 (2022); doi: 10.1063/5.0098782

Submitted: 12 May 2022 • Accepted: 4 August 2022 •

Published Online: 29 August 2022



View Online



Export Citation



CrossMark

L. Schrottke,^{1,a)} X. Lü,¹ K. Biermann,¹ P. Gellie,² and H. T. Grahn¹

AFFILIATIONS

¹ Paul-Drude-Institut für Festkörperelektronik, Leibniz-Institut im Forschungsverbund Berlin e. V., Hausvogteiplatz 5–7, 10117 Berlin, Germany

² Lytid SAS, 6 Boulevard Dubreuil, 91400 Orsay, France

^{a)} Author to whom correspondence should be addressed: lutz@pdi-berlin.de

ABSTRACT

We have investigated high-performance GaAs/AlAs terahertz (THz) quantum-cascade lasers (QCLs) with respect to the long-term stability of their operating parameters. The output power of lasers that contain an additional, thick AlAs refractive-index contrast layer underneath the cascade structure decreases after three months by about 35%. The deterioration of these lasers is attributed to the oxidation processes in this contrast layer starting from the facets. However, GaAs/AlAs THz QCLs with an $\text{Al}_{0.9}\text{Ga}_{0.1}\text{As}$ refractive-index contrast layer exhibit long-term stability of the operating parameters over many years even when they are exposed to atmospheric conditions. Therefore, these lasers are promising high-power radiation sources in the terahertz spectral region for commercial applications.

© 2022 Author(s). All article content, except where otherwise noted, is licensed under a Creative Commons Attribution (CC BY) license (<http://creativecommons.org/licenses/by/4.0/>). <https://doi.org/10.1063/5.0098782>

I. INTRODUCTION

Terahertz (THz) quantum-cascade lasers (QCLs)¹ are promising radiation sources for a number of imaging² and spectroscopic applications.³ In particular, for high-resolution spectroscopy of molecules, atoms, and ions utilizing rotational or fine-structure transitions, THz QCLs operated in the continuous-wave (cw) mode are rather unrivaled due to their narrow line widths. In atmospheric science, for example, the rotational transition of the hydroxyl radical (OH) at 3.55 THz and the fine-structure line of atomic oxygen (OI) at 4.75 THz are of interest, which can be measured with QCL-based heterodyne receivers.^{4–6} For fundamental research and industrial applications, absorption spectroscopy based on fine-structure transitions in Al, N⁺, and O at 3.36, 3.92, and 4.75 THz, respectively, is expected to allow for the quantitative determination of the atom and ion densities in plasma processes.

Although THz QCLs have to be operated at cryogenic temperatures, they have already been employed in the local oscillator for the 63-μm channel in the German REceivers for Astronomy at Terahertz frequencies (GREAT and upGREAT) on board of the Stratospheric Observatory For Infrared Astronomy (SOFIA) since 2014 to detect interstellar atomic oxygen.⁷ These applications have become possible since THz QCLs can be operated in mechanical coolers free of

cryogenic liquids.⁸ Currently, the lasers allow for cw output powers of about 10 mW and for operating temperatures of up to 75 K when operated in a miniature cooler.⁹ For less demanding applications where pulsed operation is sufficient, operating temperatures of up to 240 K have been reported but with rather small output powers well below the milliwatt level.^{10,11}

For many applications such as the illumination of microbolometer cameras with 90 000 pixels, the pumping of Schottky mixers, local oscillators in multichannel THz heterodyne spectrometers, and gas sensing, lasers with an output power of about 1 mW in cw operation are required. Therefore, we have defined the *practical operating temperature*¹² as a parameter to evaluate THz QCLs with respect to their applicability. This temperature is the maximum temperature at which a power of 1 mW is emitted. Recently, a value of 76 K has been reported for a laser with an additional mirror at the back facet.⁹ Current values reach up to 78 K even for bare lasers without a back-facet mirror (unpublished). To facilitate additional applications of THz QCLs, the practical operating temperature has to be increased, for instance, for operation in liquid-nitrogen-based coolers or to about 100 K for satellite-based instruments relying on passive cooling. Furthermore, the cooling requirements have to be reduced by improving the wall plug efficiency. These goals can be achieved by the development

of sophisticated resonator configurations for small threshold gain and improved beam geometry.^{13–15} However, straightforward waveguide and resonator structures are preferred for practical applications. Fabry-Pérot resonators based on the so-called surface plasmon waveguides¹ allow for rather large output powers and a near-Gaussian beam profile using a single lens. This approach requires an increase in the (temperature-dependent) gain of the active regions and/or a reduction in the pump power for rather large gain values, which can basically be achieved by improving the design of the active region of the QCLs.

For cw operation, hybrid designs^{16–18} have been shown to be advantageous for higher output powers using straightforward resonator configurations⁹ and for higher operating temperatures.¹⁹ In contrast, high-temperature pulsed operation relies currently on resonant-phonon designs with a smaller number of quantum wells in one period.^{10,11} A significant part of the design consideration is the conduction band offset, i.e., the barrier height. For GaAs-based QCLs, it is determined by the Al mole fraction x of the $\text{Al}_x\text{Ga}_{1-x}\text{As}$ layers. The majority of designs employ the initial composition of $x = 0.15$.^{1,20} For QCLs operating at about 2 THz, a design with a reduced Al concentration of $x = 0.1$ was reported,²¹ which was expected to render the design less sensitive to fluctuations in the growth rate and to reduce interface roughness scattering. In contrast, higher barriers with $x = 0.25$ in a hybrid design were shown to reduce the threshold current density by reducing leakage currents.²² In another study, the optimum Al concentration with respect to the highest operating temperature of resonant-phonon designs was found to be $x = 0.21$ out of a series with $0.12 \leq x \leq 0.24$.²³ Recently, the high-temperature pulsed operation up to 240 K of a THz QCL based on a resonant-phonon design was achieved using an Al mole fraction of $x = 0.3$.¹¹

In 2016, cw operation of QCLs for 4.75 THz based on GaAs/AlAs heterostructures, i.e., $x = 1.0$, was demonstrated.²⁴ The application of nominally binary AlAs barriers, which are the highest ones in the GaAs/(Al,Ga)As materials system, to QCLs of the hybrid design allows for a significantly larger wall plug efficiency than for their GaAs/ $\text{Al}_{0.25}\text{Ga}_{0.75}\text{As}$ counterparts. Meanwhile, the frequencies accessible for these lasers have been extended to the range from about 3.4 to about 5.0 THz.¹² Furthermore, the highest practical operating temperature for THz QCLs of 78 K has been achieved using GaAs/AlAs lasers. However, the growth of the AlAs layers by molecular beam epitaxy (MBE), which are necessarily very thin to compensate for the large barrier height, is rather challenging.

In addition to that, AlAs is known to oxidize as soon as it is in contact with oxygen. This oxidation process can be strongly suppressed by adding a few percent of GaAs to yield an AlAs-rich (Al,Ga)As ternary alloy or by decreasing the thickness of the AlAs layer to about or below 10 nm.²⁵ Correspondingly, GaAs/AlAs superlattices are known to be stable even over a long period of time although a possible oxidation would start at the facets immediately after cleaving the samples. These superlattices have been extensively used for decades. Even rather sophisticated effects such as the coherence resonance in a noise-driven superlattice were studied²⁶ so that we do not expect severe degradation in our lasers. Nevertheless, the long-term stability of GaAs/AlAs THz QCLs has to be verified, in particular as they are already used in the TeraCascade source from Lytid and may be candidates for implementation in satellite-based instruments.

II. EXPERIMENTAL DETAILS

For the long-term stability analysis, we used the QCL investigated in Ref. 24 (QCL A). The lasers were grown by molecular beam epitaxy. Fluctuations in the growth rates are below 1% due to a closed-loop growth rate control system based on optical reflection measurements^{27,28} for *in situ* growth control. The cascaded, active region is embedded between two highly doped GaAs contact layers. The samples were processed by photolithography and standard wet chemical etching for the (Al,Ga)As materials system using an identical procedure for all lasers. The etching solution is $\text{H}_2\text{SO}_4:\text{H}_2\text{O}_2:\text{H}_2\text{O}$ (1:1:8). The metal contacts were made from $\text{Ni}/\text{Au}_{0.995}\text{Ge}_{0.005}$ (10/150 nm) and annealed at 450 °C in order to achieve ohmic contacts. The lasers are operated in a helium flow cryostat (Oxford Optistat CF-V). The lasing spectra are measured using a Fourier-transform infrared spectrometer Bruker IFS 66v/s (original measurement) and Bruker Vertex 80v (long-term measurement) using identical resolution, while the optical power of all lasers was determined using the same power meter, Laserprobe RkP-575 RF, which was calibrated for the THz spectral range by the German National Metrology Institute (Physikalisch-Technische Bundesanstalt).²⁹ The measurements of the output power-current density-voltage (L - I - V) characteristics were repeated at several points in time over a total period of more than 6 years.

For the implementation of the *in situ* growth control based on spectroscopic methods,²⁸ an additional layer between the substrate and QCL structure is required in order to provide a contrast for the refractive index. This layer is usually an $\text{Al}_x\text{Ga}_{1-x}\text{As}$ layer with a high Al mol fraction of $x = 0.9$ and a thickness of 110 nm. However, the thermal resistivity of $\text{Al}_{0.9}\text{Ga}_{0.1}\text{As}$ has been shown to be larger by a factor of about 4 than the value for pure AlAs due to point-defect scattering of phonons.³⁰ Therefore, this layer constitutes a barrier for heat transport, which would affect the thermal management of THz QCLs. Since thermal management is an important requirement for cw operation, the $\text{Al}_{0.9}\text{Ga}_{0.1}\text{As}$ layer was replaced by a 300-nm-thick, purely binary AlAs refractive-index contrast layer for several lasers. In addition to that, the growth of the thick binary layer was also intended to determine the AlAs growth rate *in situ*. However, the rather bulky AlAs layer is even more subject to oxidation and may cause a structural damage and, hence, deterioration of the operating parameters of the lasers. To evaluate the effect of the thick AlAs layer on the properties of THz QCLs, we also investigated a pair of lasers based on the improved design used for the high-power laser operated in the miniature cooler,⁹ one of them with an AlAs layer for the refractive-index contrast (QCL B1) and one with an $\text{Al}_{0.9}\text{Ga}_{0.1}\text{As}$ layer (QCL B2).

III. RESULTS AND DISCUSSION

To examine the long-term stability of GaAs/AlAs THz QCLs, we first investigated QCL A, which contains an $\text{Al}_{0.9}\text{Ga}_{0.1}\text{As}$ contrast layer. Figure 1(a) shows the L - J - V characteristics of this laser measured directly after preparation as well as after 683 and 2241 days. For this study, the lasers were operated in the pulsed mode with pulse lengths of 500 ns in order to avoid effects resulting from a possible degradation of the thermal contact between the laser and the submount. For cw operation, this process would

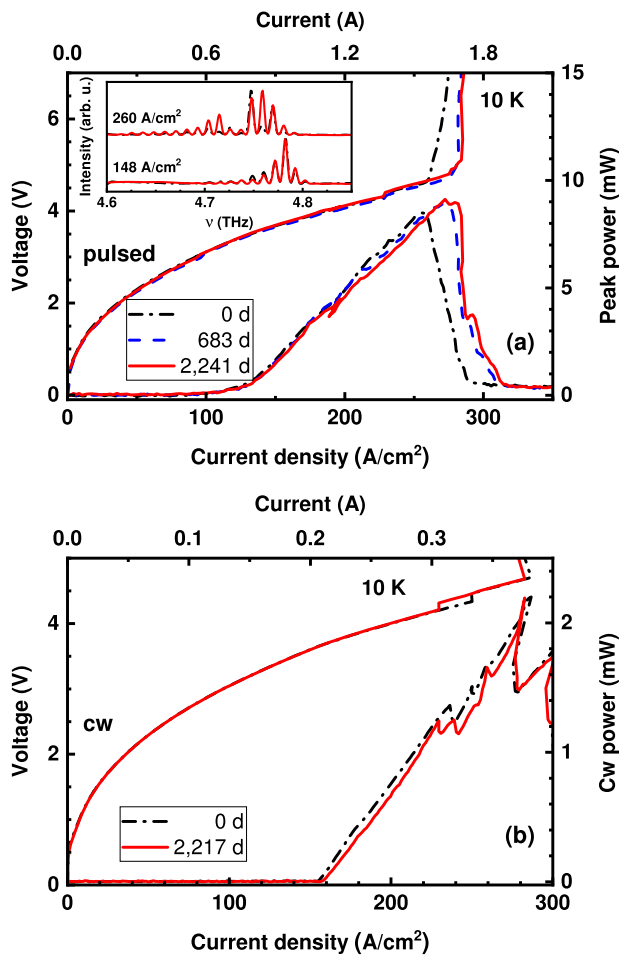


FIG. 1. (a) L - J - V characteristics for QCL A measured directly after preparation (0 days, dashed-dotted line), after 683 days (dashed line), and after 2241 days (solid line) for pulsed operation with a pulse length of 500 ns and a repetition rate of 5 kHz at a heat sink temperature of 10 K. The ridge size is $200 \times 3001 \mu\text{m}^2$. The inset shows two typical spectra at current densities as indicated after 0 and 2241 days. (b) L - J - V characteristics for QCL A measured directly after preparation (0 days, dashed-dotted line) and after 2217 days (solid line) for cw operation at a heat sink temperature of 10 K. The ridge size is $120 \times 1110 \mu\text{m}^2$.

lead to a reduction in the output power, which could not be distinguished from effects due to the degradation of the active region of the QCL. As clearly shown in Fig. 1(a), both the voltage-current density and the output power-current curves are identical within the measurement precision except for a shift in the onset of negative differential conductivity to a larger current density after 683 days. This shift may be explained by a degradation of the contacts as current instabilities are expected to react very sensitively to the contact quality. As shown in the inset of Fig. 1(a), the spectra do not show a significant change over the entire period of time. This behavior clearly shows that this GaAs/AlAs THz QCL exhibits very good long-term stability, although the nominally binary AlAs layers are exposed to atmosphere for all facets

(front, back, and two side facets) due to storage in a standard cabinet without any particular protection measures. As shown in Fig. 1(b), the lasers exhibit similar long-term stability over the entire period of six years when operated in cw mode provided that the thermal contact between the laser bar and the submount is stable as well.

The thin, nominally binary barriers consist actually of ternary compounds due to Ga and Al intermixing during growth. Recently, we have shown that the maximum Al mole fraction of the barriers in typical GaAs/AlAs THz QCLs is below 60%,³¹ i.e., a significant amount of Ga atoms is incorporated, which may prevent the oxidation of the nominally binary AlAs layers. In contrast, the AlAs refractive-index contrast layer underneath the cascade structure is buried so that it is mainly exposed to atmospheric conditions at the front and back facets; however, it is sufficiently thick to consist in its core part of binary AlAs, which is expected to oxidize quickly. Figure 2 shows optical micrographs of the front facets of QCL B1 and QCL B2. The oxidation of the AlAs refractive-index contrast layer of QCL B1 is clearly visible due to the gray stripe underneath the laser ridge, which is indicated by white arrows, while the facet area directly at the laser ridge does not show any modification. However, the $\text{Al}_{0.9}\text{Ga}_{0.1}\text{As}$ refractive-index contrast layer cannot be visually identified on QCL B2 at all.

To investigate whether the oxidation of the AlAs refractive-index contrast layers affects the operating parameters of the QCLs, we compare the L - J - V characteristics of QCL B1 and QCL B2, shown in Fig. 3. While the voltage-current density characteristics

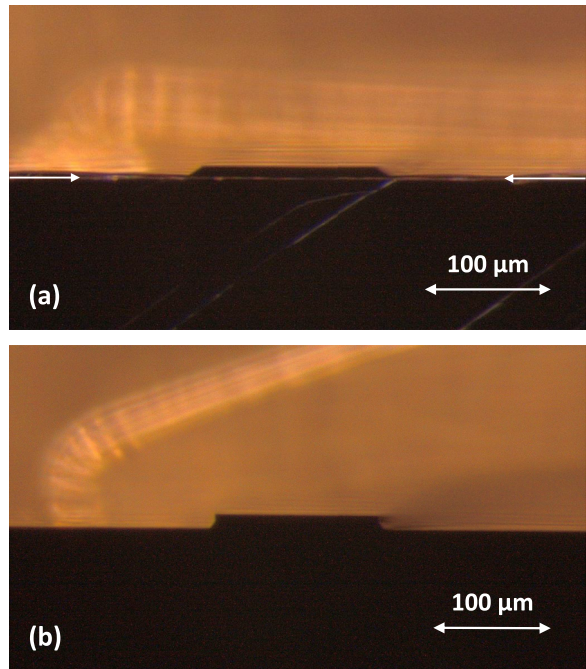


FIG. 2. Optical micrographs of the front facets of (a) QCL B1 and (b) QCL B2. The gapless gray line, which is marked by the two white arrows and is visible underneath the laser ridge and the bottom contact in (a), is attributed to the oxidized AlAs layer.

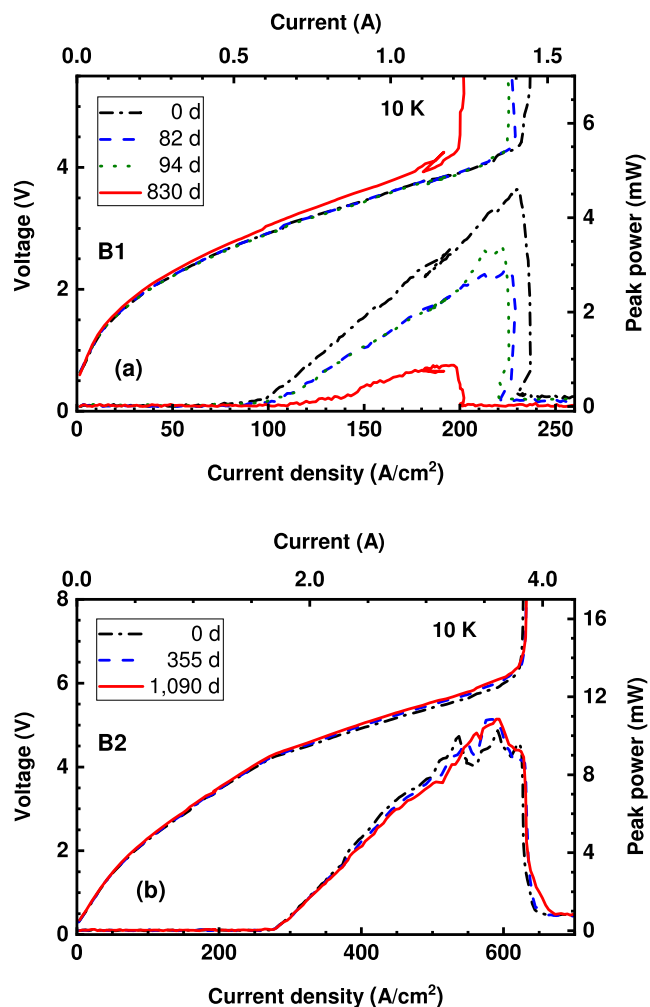


FIG. 3. (a) $L\text{-}J\text{-}V$ characteristics for QCL B1 measured directly after preparation (0 days, dashed-dotted line), after 82 days (dashed line), 94 days (dotted line), and 830 days (solid line) for pulsed operation with a pulse length of 500 ns and a repetition rate of 5 kHz at a heat sink temperature of 10 K. The ridge size is $200 \times 3051 \mu\text{m}^2$. (b) $L\text{-}J\text{-}V$ characteristics for QCL B2 measured directly after preparation (0 days, dashed-dotted line), after 355 days (dashed line), and 1090 days (solid line) for pulsed operation with a pulse length of 500 ns and a repetition rate of 5 kHz at a heat sink temperature of 10 K. The ridge size is $200 \times 3054 \mu\text{m}^2$.

appear to be rather stable for both lasers within the first 100 days, the output power of QCL B1 decreased after about three months by about 35%. After more than two years, both the transport and the optical properties have significantly changed. The current density shrunk by about 20%, while the maximum output power dropped by almost 80%. In contrast, the output power of QCL B2 remains after almost three years at the initial level just after preparation, which confirms once more that the GaAs/AlAs THz QCLs with very thin AlAs layers are stable over long operating periods. The degradation of the optical properties for lasers that have a (thick) AlAs layer underneath the active region may be attributed to the formation of

structural defects induced by strain due to the oxide,³² leading to an increase in optical losses in the waveguide. Such an increase has already been reported for oxidized, mid-infrared GaAs/AlAs waveguide structures.³³ The structural defects may penetrate into the bottom contact layer, resulting in a reduced conductivity of this contact, which may explain the reduced current density for QCL B1 after 830 days. Finally, if the defects also penetrate into the active region, the formation of possible additional states could lead to additional non-radiative transitions due to increased carrier scattering. A more detailed study of those processes in THz QCLs with AlAs refractive-index contrast layers is beyond the scope of this paper, since only lasers with $\text{Al}_{0.9}\text{Ga}_{0.1}\text{As}$ refractive-index contrast layers are useful for long-term applications.

IV. CONCLUSIONS

We have investigated GaAs/AlAs THz QCLs that contain either a thick $\text{Al}_{0.9}\text{Ga}_{0.1}\text{As}$ or a thick AlAs refractive-index contrast layer underneath the active region with respect to the long-term stability of their operating parameters. The output power of lasers with an AlAs refractive-index contrast layer decreases significantly after a few weeks, which is attributed to the oxidation processes in this layer starting from the facets. In contrast, lasers with an $\text{Al}_{0.9}\text{Ga}_{0.1}\text{As}$ contrast layer exhibit long-term stability of the operating parameters over many years even when they are exposed to atmospheric conditions. We conclude that such GaAs/AlAs THz QCLs can be used as high-quality radiation sources for commercial applications.

ACKNOWLEDGMENTS

The authors would like to thank W. Anders, M. Höricke, A. Riedel, and A. Tahraoui for sample preparation and T. Flissikowski for careful reading of the manuscript.

AUTHOR DECLARATIONS

Conflict of Interest

The authors have no conflicts to disclose.

Author Contributions

L. Schrottke: Conceptualization (lead); Methodology (equal); Project administration (equal); Writing – original draft (lead); Writing – review & editing (equal). **X. Lü:** Investigation (equal); Methodology (equal); Writing – review & editing (equal). **K. Biermann:** Investigation (equal); Methodology (equal); Writing – review & editing (equal). **P. Gellie:** Investigation (equal); Writing – review & editing (equal). **H. T. Grahn:** Project administration (equal); Resources (lead); Writing – review & editing (equal).

DATA AVAILABILITY

The data that support the findings of this study are available within the article.

REFERENCES

- ¹R. Köhler, A. Tredicucci, F. Beltram, H. E. Beere, E. H. Linfield, A. G. Davies, D. A. Ritchie, R. C. Iotti, and F. Rossi, *Nature* **417**, 156 (2002).
- ²P. Dean, A. Valavanis, J. Keeley, K. Bertling, Y. L. Lim, R. Alhathloul, A. D. Burnett, L. H. Li, S. P. Khanna, D. Indjin, T. Taimre, A. D. Rakić, E. H. Linfield, and A. G. Davies, *J. Phys. D: Appl. Phys.* **47**, 374008 (2014), and references therein.
- ³H.-W. Hübers, H. Richter, and M. Wienold, *J. Appl. Phys.* **125**, 151401 (2019), and references therein.
- ⁴J. R. Gao, J. N. Hovenier, Z. Q. Yang, J. J. A. Baselmans, A. Baryshev, M. Hajenius, T. M. Klapwijk, A. J. L. Adam, T. O. Klaassen, B. S. Williams, S. Kumar, Q. Hu, and J. L. Reno, *Appl. Phys. Lett.* **86**, 244104 (2005).
- ⁵H.-W. Hübers, S. G. Pavlov, A. D. Semenov, R. Köhler, L. Mahler, A. Tredicucci, H. E. Beere, D. A. Ritchie, and E. H. Linfield, *Opt. Express* **13**, 5890 (2005).
- ⁶L. Schrottke, M. Wienold, R. Sharma, X. Lü, K. Biermann, R. Hey, A. Tahraoui, H. Richter, H.-W. Hübers, and H. T. Grahn, *Semicond. Sci. Technol.* **28**, 035011 (2013).
- ⁷H. Richter, M. Wienold, L. Schrottke, K. Biermann, H. T. Grahn, and H.-W. Hübers, *IEEE Trans. Terahertz Sci. Technol.* **5**, 539 (2015).
- ⁸H. Richter, M. Greiner-Bär, S. G. Pavlov, A. D. Semenov, M. Wienold, L. Schrottke, M. Giehler, R. Hey, H. T. Grahn, and H.-W. Hübers, *Opt. Express* **18**, 10177 (2010).
- ⁹T. Hagelschuer, H. Richter, M. Wienold, X. Lü, B. Röben, L. Schrottke, K. Biermann, H. T. Grahn, and H.-W. Hübers, *IEEE Trans. Terahertz Sci. Technol.* **9**, 606 (2019).
- ¹⁰L. Bosco, M. Franckié, G. Scalari, M. Beck, A. Wacker, and J. Faist, *Appl. Phys. Lett.* **115**, 010601 (2019).
- ¹¹A. Khalatpour, A. K. Paulsen, C. Deimert, Z. R. Wasilewski, and Q. Hu, *Nat. Photonics* **15**, 16 (2021).
- ¹²L. Schrottke, X. Lü, B. Röben, K. Biermann, T. Hagelschuer, M. Wienold, H.-W. Hübers, M. Hannemann, J. H. van Helden, J. Röpcke, and H. T. Grahn, *IEEE Trans. Terahertz Sci. Technol.* **10**, 133 (2020).
- ¹³L. Bosco, C. Bonzon, K. Ohtani, M. Justen, M. Beck, and J. Faist, *Appl. Phys. Lett.* **109**, 201103 (2016).
- ¹⁴C. A. Curwen, J. L. Reno, and B. S. Williams, *Appl. Phys. Lett.* **113**, 011104 (2018).
- ¹⁵C. A. Curwen, J. L. Reno, and B. S. Williams, *Appl. Phys. Lett.* **116**, 241103 (2020).
- ¹⁶R. Köhler, A. Tredicucci, C. Mauro, F. Beltram, H. E. Beere, E. H. Linfield, A. G. Davies, and D. A. Ritchie, *Appl. Phys. Lett.* **84**, 1266 (2004).
- ¹⁷G. Scalari, N. Hoyler, M. Giovannini, and J. Faist, *Appl. Phys. Lett.* **86**, 181101 (2005).
- ¹⁸M. Wienold, L. Schrottke, M. Giehler, R. Hey, W. Anders, and H. T. Grahn, *Electron. Lett.* **45**, 1030 (2009).
- ¹⁹M. Wienold, B. Röben, L. Schrottke, R. Sharma, A. Tahraoui, K. Biermann, and H. T. Grahn, *Opt. Express* **22**, 3334 (2014).
- ²⁰S. Kumar, C. W. I. Chan, Q. Hu, and J. L. Reno, *Appl. Phys. Lett.* **95**, 141110 (2009).
- ²¹C. Worrall, J. Alton, M. Houghton, S. Barbieri, H. E. Beere, D. Ritchie, and C. Sirtori, *Opt. Express* **14**, 171 (2006).
- ²²M. Wienold, L. Schrottke, M. Giehler, R. Hey, W. Anders, and H. T. Grahn, *Appl. Phys. Lett.* **97**, 071113 (2010).
- ²³M. A. Kainz, S. Schönhuber, A. M. Andrews, H. Detz, B. Limbacher, G. Strasser, and K. Unterrainer, *ACS Photonics* **5**, 4687 (2018).
- ²⁴L. Schrottke, X. Lü, G. Rozas, K. Biermann, and H. T. Grahn, *Appl. Phys. Lett.* **108**, 102102 (2016).
- ²⁵K. D. Choquette, K. M. Geib, C. I. H. Ashby, R. D. Tweten, O. Blum, H. Q. Hou, D. M. Follstaedt, B. E. Hammons, D. Mathes, and R. Hull, *IEEE J. Sel. Top. Quantum Electron.* **3**, 916 (1997).
- ²⁶Y. Huang, H. Qin, W. Li, S. Lu, J. Dong, H. T. Grahn, and Y. Zhang, *Europhys. Lett.* **105**, 47005 (2014).
- ²⁷A. W. Jackson, P. R. Pusukanjana, A. C. Gossard, and L. A. Coldren, *IEEE J. Sel. Top. Quantum Electron.* **3**, 836 (1997).
- ²⁸K. Biermann, P. L. J. Helgers, A. Crespo-Poveda, A. S. Kuznetsov, A. Tahraoui, B. Röben, X. Lü, L. Schrottke, P. V. Santos, and H. T. Grahn, *J. Cryst. Growth* **557**, 125993 (2021).
- ²⁹Power values are not corrected for window transmission losses or collection efficiencies and are a lower bound by a factor of about two to the absolute power of the lasers.
- ³⁰M. A. Afromowitz, *J. Appl. Phys.* **44**, 1292 (1973).
- ³¹X. Lü, E. Luna, L. Schrottke, K. Biermann, and H. T. Grahn, *Appl. Phys. Lett.* **113**, 172101 (2018).
- ³²K. D. Choquette, K. M. Geib, H. C. Chui, B. E. Hammons, H. Q. Hou, T. J. Drummond, and R. Hull, *Appl. Phys. Lett.* **69**, 1385 (1996).
- ³³E. Guillotet, C. Langlois, M. Savanier, F. Ghiglino, S. Ducci, I. Favero, and G. Leo, *Proc. SPIE* **7728**, 772808 (2010).